Colloids and Surfaces B: Biointerfaces 162 (2018) 220–227

Contents lists available at ScienceDirect

Colloids and Surfaces B: Biointerfaces

journal homepage: www.elsevier.com/locate/colsurfb

Protocols

Participation of copper ions in formation of alginate conditioning layer: Evolved structure and regulated microbial adhesion

Xiaoyan He, Leila Abdoli, Hua Li*

Key Laboratory of Marine Materials and Related Technologies, Zhejiang Key Laboratory of Marine Materials and Protective Technologies, Ningbo Institute of Materials Technology and Engineering, Chinese Academy of Sciences, Ningbo 315201, China

ARTICLE INFO

Article history:
Received 21 August 2017
Received in revised form 21 October 2017
Accepted 23 November 2017
Available online 24 November 2017

Keywords:
Conditioning layer
Alginate
Copper alginate
Biofouling
Electron microscopy

ABSTRACT

Antifouling function of copper-based layers is usually gained through the release of cuprous or copper ions to damage most fouling species. In this research the intervening mechanisms of copper ions in formation of simplified conditioning layer comprising marine polysaccharide alginate and subsequent adhesion of typical marine bacteria and algae were studied. Fast interaction of Cu^{2+} with alginate with the formation of copper alginate multimers was observed for the first time by negative-staining electron microscopy. Interconnecting chains of alginate and copper alginate upon adsorption on silicon wafer and tangled structure of the conditioning layer were further characterized by atomic force microscopy. Adhesion testing showed that consumption of copper ions by their linking with alginate in incubation solutions resulted in mitigated toxicity of the ions to the microorganisms *Bacillus* sp., *Chlorella pyrenoidosa* and *Phaeodactylum tricornutum*. The results would give insight into understanding and regulating the formation of conditioning layer for desired antifouling performances.

1. Introduction

Biofouling is ubiquitous in the marine environment, causing severe problems such as increased operating costs, fuel consumption and CO_2 emission [1,2]. Varieties of techniques have been developed to alleviate or prevent occurring of biofouling, among which construction of superhydrophilic or superhydrophobic coatings [3], photocatalytic coatings [4], and enzyme-based antifouling coatings [5] was already reported. Yet, due to complexity of the marine environment and diversity of the fouling organisms, challenges persist in developing antifouling techniques with favorable universality and sustainability, for biofouling is a complex process involving many factors [6,7]. To date, painting with the use of biocides remains as the most effective approach to attain antifouling performances [8]. In response to the banned use of TBT-containing coatings [9], Cu-based antifouling coatings recaptured extensive attention [10]. In fact, copper plates used on vessel hulls were documented as the first antifouling devices combating formation of biofilm [8,10]. Copper and copper-based coatings are the most commonly used broad-spectrum antifouling layers due to the toxicity of copper to marine organisms [10–12]. Understanding at molecular level the antifouling mechanisms of copper is therefore essential for developing copper-related antifouling technology for widespread applications.

It is established that antifouling performances of copper-based coatings are achieved primarily through the release of cuprous and copper ions by reaction of copper with Cl^- in seawater [13]. Copper is usually harmful to microorganisms at elevated concentrations in water [10,14]. It has been reported that the toxicity usually prevails through several regimes. Copper results in different algal cell dysfunctions such as inhibition of photosynthesis, suppression of cell division, and increase of membrane permeability for algae [15]. In addition, negative effect of copper on acid-base equilibrium and ammonia excretion for marine fish and invertebrates was also reported [16]. It is noted however that the copper-associated toxicity varies depending on microorganism species and might be affected by many other factors. Knowledge about influence of copper ions on early stages of biofouling, for instance formation of conditioning layer and subsequent biofilm, is yet lacking. Moreover, there has been no report available on direct visualization of the interaction of marine biomolecules with Cu^{2+} and the interaction keeps elusive. Synergistic effect brought about by marine biomolecules and copper ions on formation of biofilm is also to be clarified.

* Corresponding author.
E-mail address: lihua@nimte.ac.cn (H. Li).

https://doi.org/10.1016/j.colsurfb.2017.11.062
0927-7765/

As typical marine polysaccharide, alginate possesses macroscopic physicochemical properties of conditioning layer [17,18]. It is a linear polysaccharide [19,20], with the capability of forming bonds with most divalent cations, such as Mg^{2+}, Ca^{2+}, Cu^{2+}, Pb^{2+} [21–24], and an egg-box interaction model for calcium alginate was already proposed [25–27]. In this study, alginate was selected as the model polysaccharide to build a simplified conditioning layer. The conditioning layer formed by the marine polysaccharide and its derivative copper alginate was examined by PeakForce quantitative nanonechanical mapping atomic force microscopy (AFM). Negative-staining electron microscopy technique was employed in this research to further characterize the conformation evolvement of copper alginate. The interaction fits the egg-box model and an interaction regime between the biomacromolecule and Cu^{2+} was proposed. Influence of copper and copper alginate on adhesion of Gram-positive bacteria (*Bacillus* sp.), diatoms (*Phaeodactylum tricornutum*), and green algae (*Chlorella pyrenoidosa*) were also investigated and elucidated.

2. Materials and methods

2.1. Sample preparation

Sodium alginate (Aladdi ustrial Corp., China) was used as received without any further purification. The M/G ratio of alginate is ~0.8 as calculated from its NMR spectrum [28]. For examination of the conditioning layer formed by alginate, appropriately diluted suspensions of sodium alginate were prepared by being dissolved in deionized water. Conditioning layer was prepared by soaking glow-discharged silicon wafers (1.0 cm × 1.0 cm) in 1 mL aqueous alginate suspension for 10 min. The samples were subsequently rinsed twice in deionized water for 5 min to remove unabsorbed alginate and then dried by flowing air at 37 °C. The alginate solution with a final concentration of 0.2 mg/mL was used for microscopy analyses. To investigate the conditioning layer formed by alginate in the presence of copper ions in the solution, the solution containing 0.1 mg/mL $CuCl_2$ and 0.2 mg/mL alginate was prepared for further experiments.

2.2. Preparation of bacterial and algal strains

Artificial seawater (ASW) was prepared according to ASTM D1141-98. All the reagents and solvents were used as received without any further purification. Gram-positive *Bacillus* sp. (MCCC1A00791, Marine Culture Collection of China) were chosen for the adhesion testing and the culturing was conducted in CM 0471-2216E media. The media were prepared by dissolving 1 g yeast extract, 1 g beef extract, 0.01 g $FePO_4$ and 5 g peptone in 1000 mL sterile ASW. The sterile media containing the bacterial strains were shaken at 25 °C at 120 rpm for 24 h. The bacteria were washed with sterile ASW for 3 times through centrifugation with a rotational speed of 2500 rpm for 5 min and then re-suspended in sterile ASW. In this work, marine strains *Chlorella pyrenoidosa* (NMBluh015-1) and *Phaeodactylum tricornutum* (NMBguh001) (Ningbo University, China) were typically chosen for the adhesion testing. *Chlorella pyrenoidosa* was cultured in filtered sterilized seawater enriched with Guillard's F/2 growth media, while *Phaeodactylum tricornutum* was cultured in sterilized seawater with silicate-enriched Guillard's F/2 growth media. The algae were cultured in an incubator with a 12 h:12 h light/dark cycle at 22 °C. The testing was carried out as they were in the exponential phase of growth.

2.3. Electron microscopy characterization

Morphology of alginate was characterized by transmission electron microscopy (TEM, FEI Tecnai F20) operated at 200 kV. For acquiring the EM images, low dose conditions (10–15 e/Å^2) were used. To investigate the interaction of Cu^{2+} with alginate, the solution containing 0.001 mg/mL $CuCl_2$ and 0.002 mg/mL alginate was prepared and excess ions were removed by dialysis. Subsequently, these solutions were used to prepare negatively stained samples by the drop by drop protocol for following TEM characterization [29]. Briefly, a 7 μL drop of prepared solution was applied to a thin carbon-coated 300-mesh copper grid. After incubating for 15 min at room temperature, the excess solution was removed by blotting with filter paper. Two consecutive drops of 7 μL 2% (w/v) uranyl acetate solution were then applied on the grid for staining. Excess stain was removed by blotting and the grid was quickly air dried at room temperature after final blotting.

2.4. AFM imaging

PeakForce quantitative nanonechanical mapping (PeakForce QNM) was performed to characterize the morphology of alginate after adsorption by using the Bruker Dimension FastScan™ AFM. The microscope was covered with an acoustic hood to minimize vibrational noise. ScanAsyst-Air cantilevers (Bruker) with a resonance frequency of 70 kHz were used and the spring constant was 0.4 N/m. Topographic height images were recorded at 1 kHz with the resolution of 1024 × 1024 pixel. All images were flattened and plane fitted by using the NanoScope Analysis software (Bruker).

2.5. Bacterial/algal adhesion testing

Bacillus sp. suspension with the bacterial concentration of 10^7 mL^{-1} was prepared in sterile ASW. Silicon wafers with three specimens for each testing group were put into 24-well plates after being ultrasonically washed with ethanol and subsequent deionized water and then dried under a flow of dried air at 37 °C. 2 mL of the *Bacillus* sp. suspension was added into each well for soaking in a shaker at 25 °C at 120 rpm for 3 days. After the incubation, the samples were washed with ASW for three times to remove the bacteria that did not adhere onto the samples and then fixed by 2.5% glutaraldehyde in ASW. Morphological features were characterized by field emission scanning electron microscopy (FESEM, FEI Quanta FEG 250). For FESEM observation, dehydration of the samples was carried out through the critical point drying using 25%, 50%, 75%, 90%, and 100% ethanol solution in turn. To clarify the synergistic influence of Cu^{2+} and alginate on the bacterial adhesion, the adhesion testing was conducted under various solution conditions, i.e. Cu^{2+}-alginate-free media, Cu^{2+}-containing media, alginate-containing media, and Cu^{2+}/alginate-containing media. The Cu^{2+}-containing media were prepared by adding 10 mM $CuCl_2$ into ASW. Concentration of alginate was 1 mg/mL in the alginate-containing ASW. The Cu^{2+}/alginate-free media were used as the control group.

2 mL algal suspension (Cu^{2+}-alginate-free media, Cu^{2+}-containing media, alginate-containing media, and Cu^{2+}/alginate-containing media) with the algal concentration of 10^6 mL^{-1} was used for the adhesion testing. Silicon wafers with 3 specimens for each testing group in 24-well plate were soaked by algal suspension in shaker for 7 days with a 12 h:12 h light/dark cycle at 22 °C. After the incubation, the wafers were washed with sterile seawater to remove the algae that did not adhere and then fixed by 2.5% glutaraldehyde in ASW for 2 h. The samples were observed by confocal laser scanning microscopy (CLSM, Leica TCS SP5, Germany).

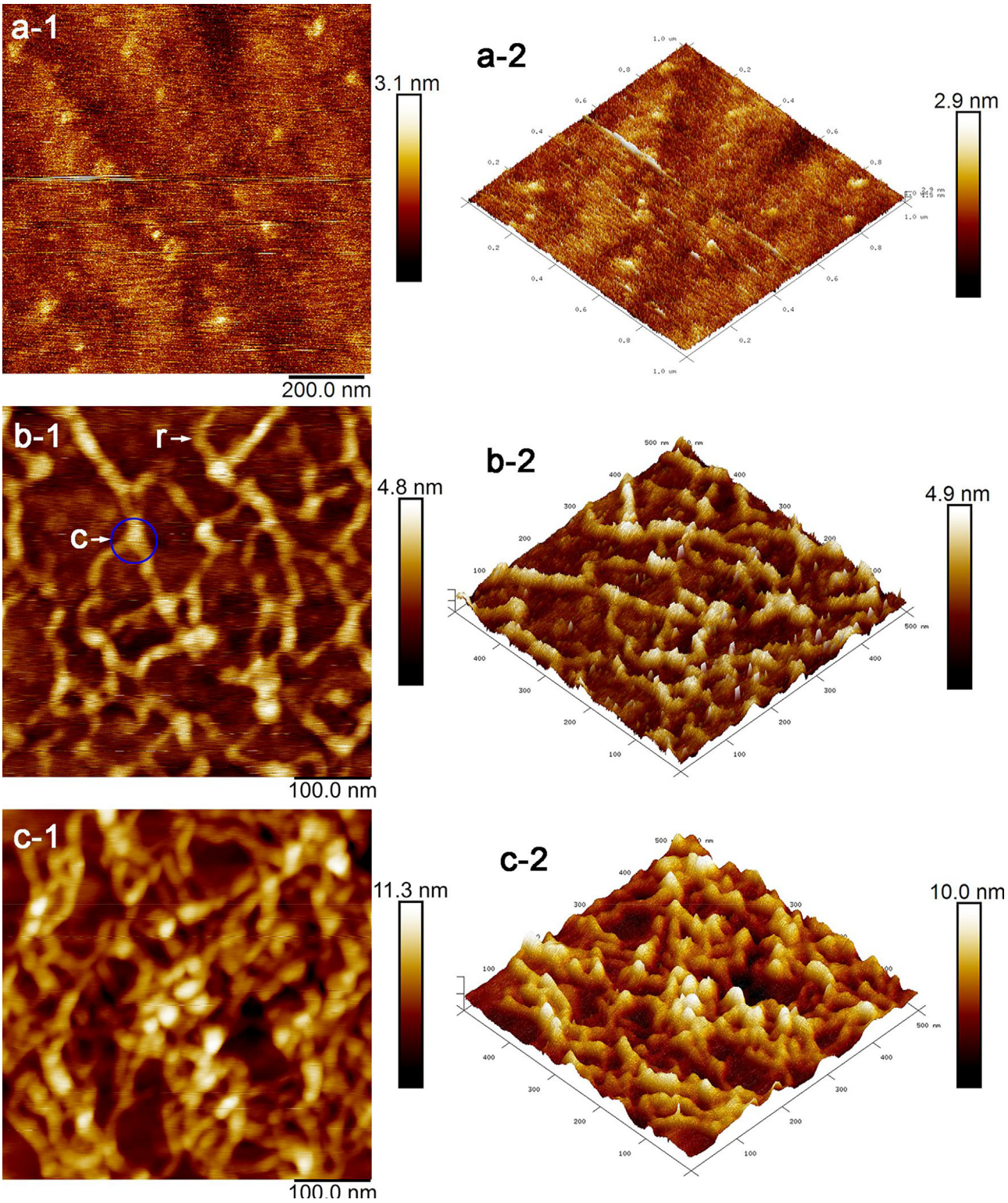

Fig 1. PeakForce QNM AFM height images (-1) and 3D images (-2) of the untreated silicon wafer (a-1, a-2), and the conditioning layer formed by alginate (b-1, b-2) and copper alginate (c-1, c-2). The rope-like morphology and the cross-linking of alginate are typically marked as r and c in (b-1).

2.6. Characterization of bacterial/algal cell-to-cell aggregation

Bacterial/algal aggregation was examined as per the previously reported protocol [30]. Settling rate of the microorganisms was measured by Lambda 950 UV/VIS spectrophotometer (PerkinElmer, USA). The bacterial suspension with a concentration of 10^7 mL^{-1} in Cu^{2+}-free and Cu^{2+}-containing ASW was mixed uniformly and then 3 mL of the suspension was transferred to cuvette for spectrophotometer measurement. OD_{600} was continuously read for 1 min to obtain the settling rate, which was calculated as the slope of the linear portion of the decreasing change in OD_{600} over time [30]. The procedures for examining algal aggregation were the same as the one used for characterizing the bacterial aggregation except

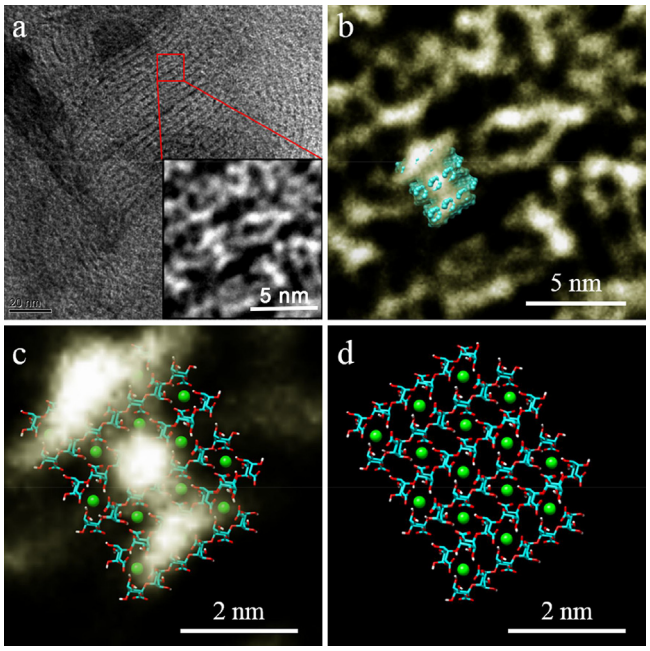

Fig. 2. Domain organization and negative-staining EM image analysis of the repeating copper alginate unit, a: the EM image shows copper alginate assembly (inset is enlarged view of selected area used for the further docking analyses), b: the selected 2D image of the molecule in agreement with surface view of the atomic structure of the egg-box of calcium alginate, indicating similar structure of copper alginate as calcium alginate, c: enlarged view of one repeating unit shows that copper alginate consists of several alginate chains connected by copper ions, and d: proposed model of the repeating copper alginate unit derived from the negative-staining EM images.

that the optical density was measured at 450 nm and the algal concentration was 10^6 mL^{-1}.

2.7. Permeability testing

For measuring the cell membrane permeability of the bacteria, the testing solution contained 20 mL *Bacillus* sp. suspension with the bacterial concentration of 10^8 mL^{-1}. Cu^{2+} with the concentration of 10 mM was added into every tube and was then mixed uniformly. At regular time intervals, 1 min, 5 min, 10 min, 30 min, 60 min, 120 min, and 180 min, the solution was mixed gently at room temperature and then allowed to stand for 1 min so that most of the cells settled out. The time intervals were usually chosen for similar study [31]. Subsequently, the samples were centrifuged for 2 min at 10,000 × *g* to remove few remaining cells. The supernatant was filtered through 0.2 μm Supor® Membrane. For each testing, control samples were directly centrifuged for 2 min at 10,000 × *g* to acquire supernatant and total leakage of the cells-containing suspension was heated at 100 °C for 5 min to provide an estimate of the total possible leakage and then centrifuged at room temperature [31]. The protein/polysaccharide content in the total extracts of *Bacillus* sp. was treated as an estimate of the total protein/polysaccharide leakage. The content of proteins and polysaccharides in the supernatant was then measured. Proteins in the testing solutions were examined using a MicroBCA protein assay reagent kit detected at 562 nm wavelength by a microplate reader (SpectraMax 190, Molecular Devices, USA), following an established protocol [32,33]. The polysaccharide content was measured by the phenol-H_2SO_4 method reported by other researchers [34,35]. Briefly, 1 mL of 6% phenol solution in ultrapure water was added into 2 mL supernatant, and immediately 5 mL 98% H_2SO_4 was added. After incubation for 20 min at room temperature, optical density of the samples was measured at 490 nm using the microplate reader. The leakage was calculated by subtracting the value of the control samples from that of the supernatant of the testing bacterial suspension.

2.8. Statistical analyses

All of the data were expressed as means ± standard deviation. Statistical analysis of *Bacillus* sp. adhering on silicon wafers was made from their SEM images acquired at a 500 × magnification. Statistical analysis of the algae adhering on silicon wafers was made by ImageJ software examination from their CLSM images with an area of 775 × 775 μm^2. Adhesion ratio is defined here as the ratio of adhesion area of the bacteria/algae to the total surface area of the substratum. The standard Student *t*-test was used to determine the difference between control and experiment groups.

3. Results and discussion

After adsorption on silicon wafer, rope-like morphology of the linear polysaccharide and linking of alginate strands is seen (Fig. 1b-1, b-2). These structural information is clear as compared to the bare silicon wafer (Fig. 1a-1, a-2). Measurement by the AFM NanoScope provides an estimate of the size of alginate strands, ~10 nm in width. This is much larger than the actual size of alginate molecule, which has been well characterized [36,37]. Apart from the probe-broadening effect caused during the AFM observation, the altered size might also indicate side-by-side association of the molecules by hydrogen bonding [37]. The measured thickness of alginate strand ranges from 0.5 nm to 1.3 nm, which is a little thicker than individual alginate chain, presumably suggesting that the individual strand is aggregate of several molecules. In addition, the tangled alginate molecules form a conditioning layer. It is speculated that the empty spaces are localized for bound and unbound water to form highly-hydrated matrix in liquid environment [38]. The conditioning layer formed by alginate holds a similar network-like structure at nanoscale as biofilm [17], which can significantly enhance or impair micro-organisms' deposition and initial adhesion, and biofilm formation through altering surface tension, charge, roughness, or hydrophobicity of substratum [18]. In addition, the alginate conditioning layer shows a Ra roughness of 0.587 nm, slightly rougher than the silicon wafer substratum, 0.347 nm.

It has been clear that alginate can bind with most divalent cations, such as Mg^{2+}, Ca^{2+}, or Cu^{2+} [22,23]. Yet study on copper alginate is rarely seen. Further AFM characterization of the adsorption of alginate on silicon wafer in the presence of Cu^{2+} reveals a layer of tangled polymeric strands (Fig. 1c-1, c-2). This suggests that addition of Cu^{2+} in the alginate-containing incubation solution facilitates adhesion of the molecules for enhanced formation of the conditioning layer. Apart from the promoted adhesion of the polysaccharides on silicon wafer, significantly increased thickness of the conditioning layer (the distance between the top layer and the substrate surface) is seen (~10 nm in Fig. 1c-2 versus ~4.9 nm in Fig. 1b-2). The conditioning layer also shows much rougher surface than the conditioning layer formed by alginate alone (Ra value of 1.17 nm versus 0.587 nm). These might suggest incorporation of Cu^{2+} into alginate chains, which in turn alters the spatial conformation of alginate. Such an arrangement would potentially contribute to a physically strongly adhered conditioning layer.

In fact, linking of Cu^{2+} with alginate is visualized by negatively stained EM analyses (Fig. 2). Our previous study already revealed the width of single-stranded alginate to be less than 1 nm [28]. After linking with copper ions, alginate molecule evolves significantly into much wider chains (Fig. 2a). Enlarged view shows clearly the morphological feature of copper alginate and provides clues of binding regime of Cu^{2+} with alginate fragment (Fig. 2b

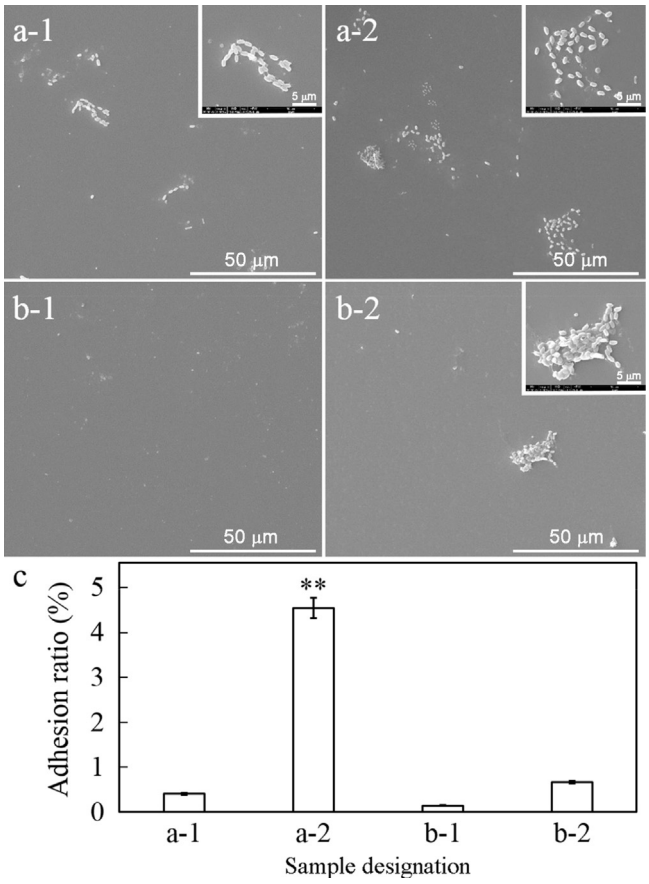

Fig. 3. SEM Images of *Bacillus* sp. adhered on silicon wafer in Cu^{2+}-alginate-free media (a-1), alginate-containing media (a-2), Cu^{2+}-containing media (b-1), and Cu^{2+}-alginate-containing media (b-2) (inset is enlarged view); and **c**: statistical analyses of the bacteria adhered on silicon wafer, error bars are shown as ±SD (n = 10). **: $p < 0.05$ as compared with the control groups.

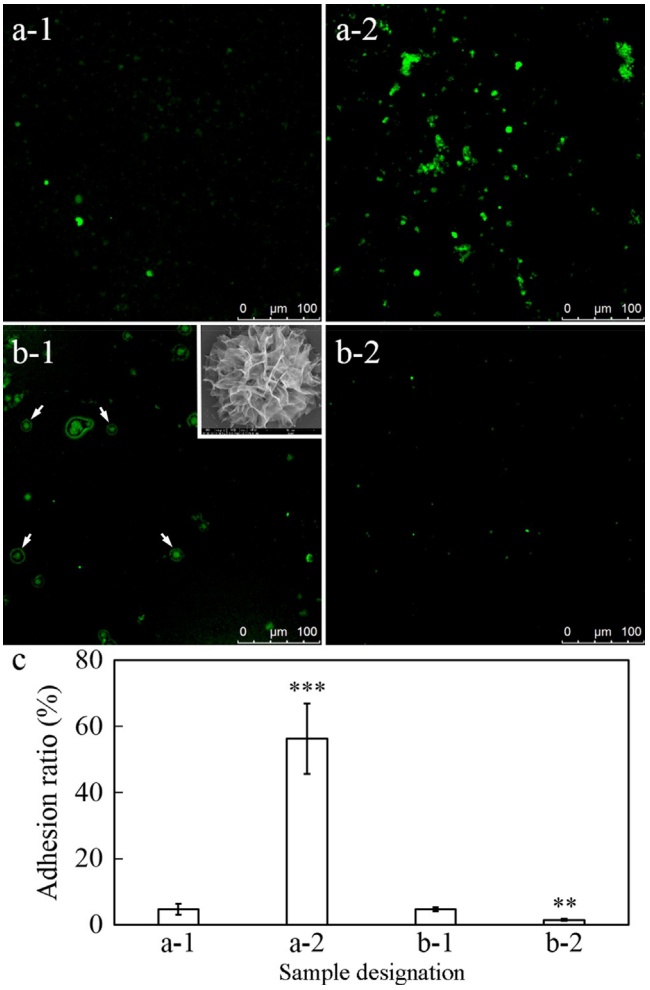

Fig. 4. CLSM imaging of *Chlorella pyrenoidosa* adhered on silicon wafer in Cu^{2+}-alginate-free media (a-1), alginate-containing media (a-2) (inset is enlarged view showing damaged morphology of the adhered *Chlorella pyrenoidosa*), Cu^{2+}-containing media (b-1), and Cu^{2+}-alginate-containing media (b-2); and **c**: statistical adhesion ratio of *Chlorella pyrenoidosa*, error bars are shown as ±SD (n = 10). **: $p < 0.05$ and ***: $p < 0.005$ as compared with the control group. The damaged *Chlorella pyrenoidosa* are typically marked by the white arrows in b-1.

and c). It is noted that the resolution is relatively low due to the staining of heavy metals during the sample preparation. An egg-box interaction model between Ca^{2+} and alginate was proposed previously [25–27]. It is believed that calcium ion was captured electrostatically by the GG block of alginate, resulting in formation of an egg-box conformation [39], and one junction zone of the calcium alginate molecular is ~0.87 nm in length [25,40,41]. Our TEM characterization suggests similar egg-box interaction for copper alginate (Fig. 2d). Copper ions might also be captured by G-blocks of alginate by electrostatic attraction, thus resulting in formation of copper alginate [42]. To elucidate the conformational changes of alginate after linking with copper ions, we managed to dock the egg-box model of calcium alginate into copper alginate (Fig. 2) by using the molecular modeling system Chimera [43]. It is surprisingly noted that the 2D EM image agrees well with the atomic structure of alginate chains containing calcium ions which was already reported [39]. The width between two copper ions in parallel lines coincides with the enlarged 2D EM image (Fig. 2 b). It is difficult to dock the atomic structure into the whole 2D EM image since the interaction already tangled multiple alginate molecules in 3D view. Our ongoing research efforts are therefore being devoted to reconstructing 3D structures of the polysaccharide. Nevertheless, this preliminary docking already provides sufficient useful clues of the structure changes of alginate, that is, linking of alginate with copper ions happened upon adsorption of the molecule. Increased size of the chains likely results from incorporation of copper ions. Interestingly, the width of copper alginate is much wider than that of calcium alginate. The electrostatic attraction between copper ions and alginate could be stronger than that for calcium ions since in nature copper ion is much smaller than calcium ion. This strong binding state might have pronounced impact on subsequent adhesion behaviors of microorganisms.

In addition, it has been noted that the “buckled” conformation leaves repeating unfilled caves in the conditioning layer (Figs. 1 and 2). The empty space might affect formation of biofilm through regulating colonization behaviors of bacteria/diatoms. After 3 days incubation in ASW, adhesion of *Bacillus* sp. on silicon wafer is observed (Fig. 3). EPS formation is obviously perceived from enlarged views (inset in Fig. 3). After the 3 days incubation, adhesion ratio of *Bacillus* sp. is 0.41%, while the ratio is significantly increased to 4.54% as alginate is added in the solution. It is therefore clear that alginate promotes the adhesion and aggregation of *Bacillus* sp. While it is not surprising that presence of Cu^{2+} in the solution deteriorates the bacterial adhesion, since the ions are toxic to the bacteria. Strikingly, it is noted that certain amount of alive bacteria still adhere on silicon wafer in the co-presence of alginate and Cu^{2+}. Mitigated toxicity of Cu^{2+} is suggested, which can be well explained by the formation of copper alginate that has readily formed upon adsorption (Figs. 1 and 2). The conditioning layer formed by copper alginate seems not to exert remarkable effect on *Bacillus* sp. adhesion.

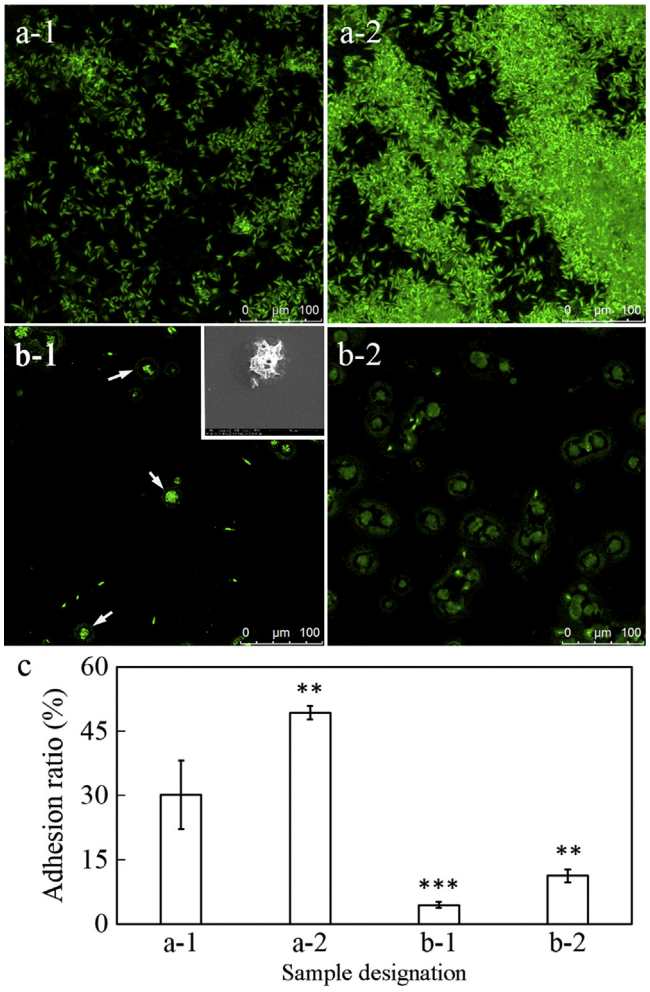

Fig. 5. CLSM imaging of *Phaeodactylum tricornutum* adhered on silicon wafer in Cu^{2+}-alginate-free media (a-1), alginate-containing media (a-2), Cu^{2+}-containing media (b-1) (inset is enlarged view of broken *Phaeodactylum tricornutum*), and Cu^{2+}-alginate-containing media (b-2); and c: statistical adhesion ratio of *Phaeodactylum tricornutum*, error bars are shown as ±SD (n = 10). **: $p < 0.05$ and ***: $p < 0.005$ as compared with the control groups. The damaged *Phaeodactylum tricornutum* are typically marked by the white arrows in b-1.

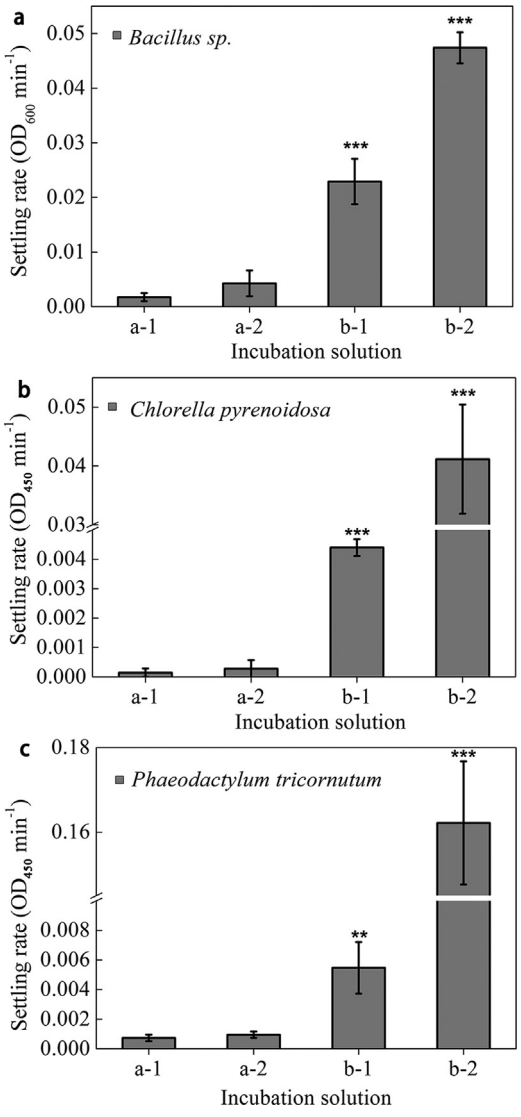

Fig. 6. Assessment of cell-to-cell aggregation by measuring the settling rate of *Bacillus sp., Chlorella pyrenoidosa* and *Phaeodactylum tricornutum* in Cu^{2+}-alginate-free media (a-1), alginate-containing media (a-2), Cu^{2+}-containing media (b-1), and Cu^{2+}-alginate-containing media (b-2). Error bars are shown as ±SD (n = 3). ***: $p < 0.005$ as compared with the control group.

Similar phenomenon is also found for *Chlorella pyrenoidosa* and *Phaeodactylum tricornutum*. After 7 days incubation in F/2-media, clear adhesion of the algae on silicon wafer is realized (Figs. 4 and 5). Presence of alginate facilitates the adhesion of *Chlorella pyrenoidosa*. Damaged morphological feature of the adhered *Chlorella pyrenoidosa* with completely broken cytomembrane in Cu^{2+}-containing media is seen (inset in Fig. 4b-1), suggesting the extinguishing effect of Cu^{2+}. Statistical analyses of the algal adhesion show that after 7 days incubation, alginate causes significant increase in adhesion ratio of *Chlorella pyrenoidosa* from 4.70% to 56.23% (Fig. 4c). This is presumably due to the fact that alginate already forms a conditioning layer with rough morphology (Fig. 1b-2), in turn facilitating the adhesion of *Chlorella pyrenoidosa*, since it is hard for ball-like *Chlorella pyrenoidosa* to adhere on substratum surface by itself. For the Cu^{2+}-containing solution, only dead *Chlorella pyrenoidosa* is seen on the surface of the substratum, suggesting pronounced damaging function of Cu^{2+}. Alginate increases the adhesion of *Phaeodactylum tricornutum* (49.30% versus 30.20%) (Fig. 5). However, adhesion of *Phaeodactylum tricornutum* turns to be worse in the presence of Cu^{2+} in the solution, dropping sharply to 4.42%, and most of them are extinguished by Cu^{2+}. Distorted *Phaeodactylum tricornutum* are seen and their cell membrane is ruptured (inset in Fig. 5b-1). Interestingly, adhered *Chlorella pyrenoidosa* algae are seen on the conditioning layer formed by copper alginate. These further evidence the finding that the conditioning layer formed by copper alginate have less toxicity to the microorganisms, due predominately to preferable consumption of toxic copper ions in unhindered state by alginate through electrostatic linking. Yet, it is noted that the conditioning layer formed by copper alginate does not promote the adhesion of the microorganisms, the few live alga look unhealthy (Fig. 5b-2).

Alginate and Cu^{2+} in the media also influence aggregation behaviors of the microorganisms. Settling rate assay was employed to assess the aggregation and enhanced settling usually corresponds to accelerated aggregation. Result shows that alginate has little influence on the settling of *Bacillus sp., Chlorella pyrenoidosa,* and *Phaeodactylum tricornutum* on the substrata, however, presence of Cu^{2+} alone or both Cu^{2+} and alginate in the solution greatly promotes their settling (Fig. 6). The ions remarkably accelerate aggregation of *Bacillus* sp. and *Chlorella pyrenoidosa* and give rise to 7.5-fold increase in sedimentation of *Phaeodactylum tricornutum*. These phenomena might be related to the impact of

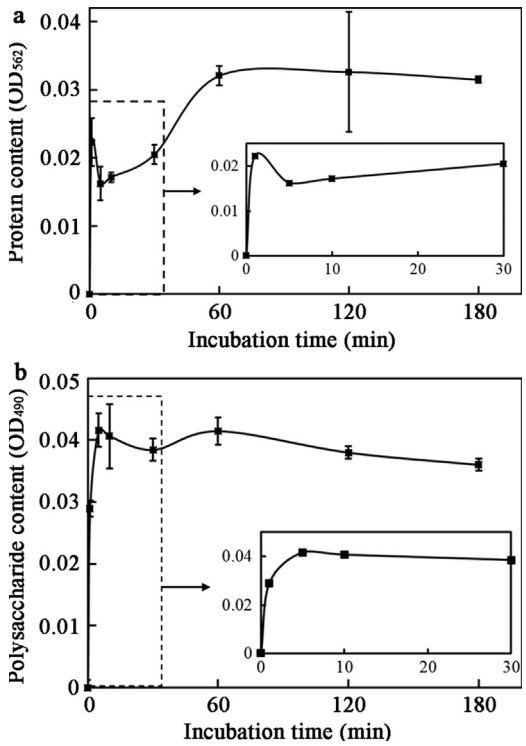

Fig. 7. Influence of the addition of copper ions on leakage of proteins (a) and polysaccharides (b) from *Bacillus* sp. after different incubation durations. Error bars are shown as ±SD (n = 3). (Inset is enlarged view of the selected plot).

copper ions on cytomembrane of the microorganisms. It is known that major components of cytomembrane, for instance polysaccharides, proteins, lipoproteins, and humic substances, are negatively charged and have many electronegative functional groups, such as carboxyl, phosphoric, sulfhydryl, and hydroxyl groups, which can bind with divalent cations mainly by intermolecular interactions [44]. We already realized that most divalent cations, such as Mg^{2+} and Ca^{2+}, facilitate aggregation of *Bacillus* sp./*Chlorella pyrenoidosa*/*Phaeodactylum tricornutum* [45], and they improve flocculation of microbial aggregates and maintain the microbial aggregate structure [30,44]. However, the coagulation ability of Cu^{2+} is much stronger than that of Mg^{2+}/Ca^{2+}, which could be attributed to the smaller radius of Cu^{2+} than Mg^{2+}/Ca^{2+}. The remarkably enhanced settling indicates presumably quick linking of Cu^{2+} with the biomacromolecule existing in cytomembrane. This strong interaction would however in turn result in increased cell permeability and ion leakage.

It is found that presence of copper ions in the incubation solution already triggered leakage of proteins and polysaccharides from *Bacillus* sp. into the media (Fig. 7). Quick leakage response is realized. The rapid increase of OD value to 0.022 is seen, which is almost 77% of the protein content in total possible leakage, 0.029. Subsequently, after addition of copper ions into the culturing solution for 5 min, the value decreases to 0.016, and then the protein content increases slowly and reaches an equilibrium after 60 min culturing, 0.032. This can be likely explained by the fact that Cu^{2+} quickly changes the cell permeability of *Bacillus* sp., causing protein leakage and then some of the proteins are adsorbed on tube surface. This phenomenon would account for the reduced protein concentration in the solution at early incubation stage. In addition, leakage of polysaccharides into the solution is also noticed (Fig. 7b). Rapid increase of the polysaccharide content in *Bacillus* sp. is seen in the initial 5 min, followed by decelerated increment. Moreover, the polysaccharide content in the initial 5 min incubation is almost 95% of that in total possible leakage (0.042 versus 0.043). For the control samples, no leakage of either proteins or polysaccharides is realized. It can therefore be claimed that copper ions triggered promoted cell permeability of *Bacillus* sp. Similar Cu^{2+}-triggered leakage of proteins/polysaccharides was also realized for *Chlorella* and *Phaeodactylum tricornutum* (data not shown).

Consumption of copper ions by their quick linking with alginate chains already mitigates their toxicity. In addition, the conditioning layer comprising copper alginate exhibits rougher surface than the alginate conditioning layer, which would in turn facilitate settling of the microorganisms (Fig. 1c-2 versus b-2). The physicochemical nature of conditioning layer is the main factor dominating adhesion of microorganisms. Our attempt of clarifying the participation of the typical divalent cations in formation of conditioning layer proves the feasibility of AFM and negatively staining EM approaches for biofouling study at molecular level.

4. Conclusions

Quick linking of copper ions with alginate was visualized for the first time by negative-staining electron microscopy. AFM characterization further revealed the network-like structure of alginate and copper alginate conditioning layer formed on silicon wafer. The interaction of alginate with copper ions consumes certain amount of the ions in solution, resulting directly in mitigated toxicity of the ions to marine microorganisms. Adhesion testing of *Bacillus* sp., *Chlorella pyrenoidosa* and *Phaeodactylum tricornutum* on silicon wafer in artificial seawater suggests that conditioning layer formed by alginate alone promotes their adhesion, while the layer formed by copper alginate shows minor influence. The settling testing of the microorganisms further suggests that Cu^{2+} has strong connection with their secreted EPS and presumably affects their cell membrane permeability.

Acknowledgments

This research was supported by National Natural Science Foundation of China (grant # 41476064, and 51401232), Key Research and Development Program of Zhejiang Province (grant # 2017C01003), and Project of Scientific Innovation Team of Ningbo (grant # 2015B11050).

References

[1] D.L. Schmidt, R.F. Brady, K. Lam, D.C. Schmidt, M.K. Chaudhury, Contact angle hysteresis, adhesion, and marine biofouling, Langmuir 20 (2004) 2830–2836.
[2] O. Andersson, T. Ekblad, N. Aldred, A.S. Clare, B. Liedberg, Novel application of imaging surface plasmon resonance for in situ studies of the surface exploration of marine organisms, Biointerphases 4 (2009) 65–68.
[3] J.Q. Flores, Y.S. Joung, N.M. Kinsinger, X. Lu, S.L. Walker, Antimicrobial behavior of novel surfaces generated by electrophoretic deposition and breakdown anodization, Colloids Surf. B 134 (2015) 204–212.
[4] R. Dineshram, R. Subasri, K.R.C. Somaraju, K. Jayaraj, L. Vedaprakash, K. Ratnam, S.V. Joshi, R. Venkatesan, Biofouling studies on nanoparticle-based metal oxide coatings on glass coupons exposed to marine environment, Colloids Surf. B 74 (2009) 75–83.
[5] S.M. Olsen, L.T. Pedersen, M.H. Laursen, S. Kiil, K. Dam-Johansen, Enzyme-based antifouling coatings: a review, Biofouling 23 (2007) 369–383.
[6] Y.H. An, R.J. Friedman, Concise review of mechanisms of bacterial adhesion to biomaterial surfaces, J. Biomed. Mater. Res. 43 (1998) 338–348.
[7] M. Katsikogianni, Y. Missirlis, Concise review of mechanisms of bacterial adhesion to biomaterials and of techniques used in estimating bacteria-material interactions, Eur. Cells Mater. 8 (2004) 37–57.
[8] A. Rosenhahn, S. Schilp, H.J. Kreuzer, M. Grunze, The role of inert surface chemistry in marine biofouling prevention, Phys. Chem. Chem. Phys. 12 (2010) 4275–4286.
[9] H.U. Dahms, X. Ying, C. Pfeiffer, Antifouling potential of cyanobacteria: a mini-review, Biofouling 22 (2006) 317–327.
[10] R.F. Piola, K.A. Dafforn, E.L. Johnston, The influence of antifouling practices on marine invasions, Biofouling 25 (2009) 633–644.
[11] T. Kruk, K. Szczepanowicz, J. Stefańska, R.P. Socha, P. Warszyński, Synthesis and antimicrobial activity of monodisperse copper nanoparticles, Colloids Surf. B 128 (2015) 17–22.

[12] M.J. Vucko, P.C. King, A.J. Poole, Y. Hu, M.Z. Jahedi, R. de Nys, Assessing the antifouling properties of cold-spray metal embedment using loading density gradients of metal particles, Biofouling 30 (2014) 651–666.
[13] D. Rui, L. Xiangbo, W. Jia, X. Likun, Electrochemical corrosion and mathematical model of cold spray Cu-Cu_2O coating in NaCl solution – part I: tafel polarization region model, Int. J. Electrochem. Sci. 8 (2013) 5902–5924.
[14] M. Grosell, J. Blanchard, K.V. Brix, R. Gerdes, Physiology is pivotal for interactions between salinity and acute copper toxicity to fish and invertebrates, Aquat. Toxicol. 84 (2007) 162–172.
[15] K.P. Tsai, Effects of two copper compounds on *Microcystis aeruginosa* cell density membrane integrity, and microcystin release, *Ecotox*, Environ. Safe 120 (2015) 428–435.
[16] T.M. Lopes, I.F. Barcarolli, C.B. de Oliveira, M.M. de Souza, A. Bianchini, Effect of copper on ion content in isolated mantle cells of the marine clam *Mesodesma mactroides*, Environ. Toxicol. Chem. 30 (2011) 1582–1585.
[17] T. Schmid, J. Burkhard, B.-S. Yeo, W. Zhang, R. Zenobi, Towards chemical analysis of nanostructures in biofilms I: imaging of biological nanostructures, Anal. Bioanal. Chem. 391 (2008) 1899–1905.
[18] G. Hwang, S. Kang, M.G. El-Din, Y. Liu, Impact of conditioning films on the initial adhesion of *Burkholderia cepacia*, Colloids Surf. B 91 (2012) 181–188.
[19] W. Li, X.Y. Li, Y. Chen, X.X. Li, H.B. Deng, T. Wang, R. Huang, G. Fan, Poly(vinyl alcohol)/sodium alginate/layered silicate based nanofibrous mats for bacterial inhibition, Carbohydr. Polym. 92 (2013) 2232–2238.
[20] F. Ding, X. Shi, S. Wu, X. Liu, H. Deng, Y. Du, H. Li, Flexible polysaccharide hydrogel with pH-regulated recovery of self-healing and mechanical properties, Macromol. Mater. Eng. (2017) 1700221.
[21] I. Donati, F. Asaro, S. Paoletti, Experimental evidence of counterion affinity in alginates: the case of nongelling ion Mg^{2+}, J. Phys. Chem. B 113 (2009) 12877–12886.
[22] T. Baumberger, O. Ronsin, Cooperative effect of stress and ion displacement on the dynamics of cross-link unzipping and rupture of alginate gels, Biomacromolecules 11 (2010) 1571–1578.
[23] C.K. Siew, P.A. Williams, N.W. Young, New insights into the mechanism of gelation of alginate and pectin: charge annihilation and reversal mechanism, Biomacromolecules 6 (2005) 963–969.
[24] C.H. Yang, M.X. Wang, H. Haider, J.H. Yang, J.Y. Sun, Y.M. Chen, J. Zhou, Z. Suo, Strengthening alginate/polyacrylamide hydrogels using various multivalent cations, ACS Appl. Mater. Interfaces 5 (2013) 10418–10422.
[25] P. Sikorski, F. Mo, G. Skjåk-Bræk, B.T. Stokke, Evidence for egg-box-compatible interactions in calcium-alginate gels from fiber X-ray diffraction, Biomacromolecules 8 (2007) 2098–2103.
[26] M. Borgogna, G. Skjak-Braek, S. Paoletti, I. Donati, On the initial Bbinding of alginate by calcium ions: the tilted egg-box hypothesis, J. Phys. Chem. B 117 (2013) 7277–7282.
[27] G.T. Grant, E.R. Morris, D.A. Rees, P.J.C. Smith, D. Thom, Biological interactions between polysaccharides and divalent cations-egg-box model, FEBS Lett. 32 (1973) 195–198.
[28] X. He, Y. Liu, H. Li, H. Li, Single-stranded structure of alginate and its conformation evolvement after an interaction with calcium ions as revealed by electron microscopy, RSC Adv. 6 (2016) 114779–114782.
[29] H. Li, M. Chavan, H. Schindelin, W.J. Lennarz, H. Li, Structure of the oligosaccharyl transferase complex at 12 Å resolution, Structure 16 (2008) 432–440.
[30] L.F. Cruz, P.A. Cobine, L. de La Fuente, Calcium increases *Xylella fastidiosa* surface attachment biofilm formation, and twitching motility, Appl. Environ. Microb. 78 (2012) 1321–1331.
[31] D.H. Young, H. Köhle, H. Kauss, Effect of chitosan on membrane permeability of suspension-cultured *Glycine max* and *Phaseolus vulgaris* cells, Plant Physiol. 70 (1982) 1449–1454.
[32] M.A. Patrauchan, S. Sarkisova, K. Sauer, M.J. Franklin, Calcium influences cellular and extracellular product formation during biofilm-associated growth of a marine *Pseudoalteromonas sp*, Microbiology 151 (2005) 2885–2897.
[33] X. Chen, K. Cai, M. Lai, L. Zhao, L. Tang, Mesenchymal stem cells differentiation on hierarchically micro/nano-structured titanium substrates, Adv. Eng. Mater. 14 (2012) B216–B223.
[34] X. Chen, S.R. Suwarno, T.H. Chong, D. Mcdougald, S. Kjelleberg, Y. Cohen, A.G. Fane, S.A. Rice, Dynamics of biofilm formation under different nutrient levels and the effect on biofouling of a reverse osmosis membrane system, Biofouling 29 (2013) 319–330.
[35] O. Orgad, Y. Oren, S.L. Walker, M. Herzberg, The role of alginate in *Pseudomonas aeruginosa* EPS adherence, biscoelastic properties and cell attachment, Biofouling 27 (2011) 787–798.
[36] H. Hecht, S. Srebnik, Structural characterization of sodium alginate and calcium alginate, Biomacromolecules 17 (2016) 2160–2167.
[37] A.W. Decho, Imaging an alginate polymer gel matrix using atomic force microscopy, Carbohyd. Res. 315 (1999) 330–333.
[38] A.W. Decho, In situ imaging and characterizing the matrix of extracellular polymeric substances (EPS) of biofilms, Microsc. Microanal. 15 (2009) 822–823.
[39] I. Braccini, R.P. Grasso, S. Pérez, Conformational and configurational features of acidic polysaccharides and their interactions with calcium ions: a molecular modeling investigation, Carbohyd. Res. 317 (1999) 119–130.
[40] W. Plazinski, Molecular basis of calcium binding by polyguluronate chains: revising the egg-box model, J. Comput. Chem. 32 (2011) 2988–2995.
[41] E.E. Urena-Benavides, C.L. Kitchens, Wide-angle X-ray diffraction of cellulose nanocrystal-alginate nanocomposite fibers, Macromolecules 44 (2011) 3478–3484.
[42] M. Grace, N. Chand, S.K. Bajpai, Copper alginate-cotton cellulose (CACC) Fibers with excellent antibacterial properties, J. Eng. Fibers Fabr. 4 (2009) 24–35.
[43] E.F. Pettersen, T.D. Goddard, C.C. Huang, G.S. Couch, D.M. Greenblatt, E.C. Meng, T.E. Ferrin, U.C.S.F. Chimera, - a visualization system for exploratory research and analysis, J. Comput. Chem. 25 (2004) 1605–1612.
[44] G.-P. Sheng, H.-Q. Yu, X.-Y. Li, Extracellular polymeric substances (EPS) of microbial aggregates in biological wastewater treatment systems: a review, Biotechnol. Adv. 28 (2010) 882–894.
[45] X. He, J. Wang, L. Abdoli, H. Li, Mg^{2+}/Ca^{2+} Promotes the adhesion of marine nacteria and algae and enhances following biofilm formation in artificial seawater, Colloids Surf. B 146 (2016) 289–295.